MolecularMedicine

The Multi-target Effects of CNI-1493: Convergence of Antiamylodogenic and Antiinflammatory Properties in Animal Models of Alzheimer's Disease

Roman Sankowski,[1,2,3] Arne Herring,[4] Kathy Keyvani,[4] Kathrin Frenzel,[1] Jinyu Wu,[2] Stephan Röskam,[5] Carmen Noelker,[6] Michael Bacher,[7] and Yousef Al-Abed[2]

[1]Institute of Neuropathology, University of Freiburg, Freiburg, Germany; [2]Center for Molecular Innovation, The Feinstein Institute for Medical Research, Manhasset, NY, United States of America; [3]Elmezzi Graduate School of Molecular Medicine, Manhasset, NY, United States of America; [4]Institute of Neuropathology, University of Duisburg-Essen, Essen, Germany; [5]Institute of Medical Sociology and Social Medicine, Philipps-University of Marburg, Marburg, Germany; [6]Department of Neurology, Faculty of Medicine, Philipps-University of Marburg, Marburg, Germany; and [7]Institute of Immunology, Philipps-University, Marburg, Germany

After several decades of Alzheimer's disease (AD) research and failed clinical trials, one can speculate that targeting a single pathway is not sufficient. However, a cocktail of novel therapeutics will constitute a challenging clinical trial. A more plausible approach will capitalize on a drug that has relevant and synergistic multiple-target effects in AD. We have previously demonstrated the efficacy of CNI-1493 in the CRND8 transgenic AD mouse model. Similar to many antiinflammatory drugs that were tested in preclinical models of AD, it was speculated that the significant effect of CNI-1493 is due to its established antiinflammatory properties in rodents and humans. In the present study, we set out to elucidate the protective mechanism of CNI-1493 as a drug simultaneously targeting several aspects of AD pathology. Using C1213, a highly similar analogue of CNI-1493 that lacks antiinflammatory properties, we show that both compounds directly interact with soluble and insoluble amyloid β (Aβ) aggregates and attenuate Aβ cytotoxicity *in vitro*. Additionally, CNI-1493 and C1213 ameliorates Aβ-induced behavioral deficits in nematodes. Finally, C1213 reduces Aβ plaque burden and cognitive deficits in transgenic CRND8 mice to a similar extent as previously shown with CNI-1493. Taken together, our findings suggest antiamyloidogenic activity as a relevant component of the in vivo efficacy of CNI-1493 and its analogue C1213. Thus, CNI-1493, a drug with proven safety in humans, is a viable candidate for novel multitarget therapeutic approaches to AD.

Online address: http://www.molmed.org
doi: 10.2119/molmed.2016.00163

INTRODUCTION

CNI-1493 is a synthetic guanylhydrazone developed as an inhibitor of cytokine-induced arginine transport and nitric oxide production in macrophages (1). In the last years, CNI-1493 has been shown to be a potent antiinflammatory agent in animal disease models and clinical studies. CNI-1493 was investigated in clinical trials for Crohn's disease as an intravenous formulation (2) and soon will be tested in an oral formulation.

CNI-1493 suppresses the production of several proinflammatory cytokines in macrophages; eg, tumor necrosis factor (TNF) and interleukin-6 (IL-6) (3). It has been shown that these inhibitory effects on cytokine production are likely due to inhibition of the mitogen-activated protein kinase (MAPK; p38, c-Jun N-terminal kinase [JNK]), extracellular-signal regulated kinase (ERK) signal transduction pathways. Impaired phosphorylation of MAPK kinases (i.e. MAPK/ERK kinase 1/2 (MEK1/2), MAPK kinase (MKK4) and MKK3/6) were seen in treatment with CNI-1493, and a direct interaction of CNI-1493 with upstream molecules was suggested but has not yet been shown (4). Preclinical studies have

Address correspondence to *Roman Sankowski, Institute of Neuropathology, University of Freiburg, Freiburg, Germany; Phone: +49 761 270 51090; Email: roman.sankowski@uniklinik-freiburg.de. Michael Bacher, Institute of Immunology, Philipps-University Marburg, Hans-Meerwein-Str, 35043 Marburg, Germany; Phone: 06421-28-65311; E-mail: bacher@staff.uni-marburg.de. Yousef Al-Abed, Center for Molecular Innovation, The Feinstein Institute for Medical Research, 350 Community Drive, Manhasset, NY 11030 USA; Phone: (516) 562-3406; E-mail: yalabed@northwell.edu.*
Submitted July 12, 2016; Accepted for Publication October 20, 2016; Published Online (www.moldmed.org) November 15, 2016.

convincingly demonstrated the efficacy of CNI-1493 in animal disease models of inflammation. For example, administration of this compound to mice conferred protection against both carrageenan-induced inflammation and lethal endotoxemia (1). CNI-1493 is now known to have beneficial effects not only in inflammatory and autoimmune diseases, but also in viral and parasitic infections (5–7). In combination with the interleukin-2 (IL-2) anti-tumor therapy, CNI-1493 could also reduce the toxic side effects in animal models, although it failed in clinical trials, likely due to formulation and route of administration issues (8,9).

These beneficial effects in systemic inflammatory disorders indicated CNI-1493 as a potential therapeutic substance for neuroinflammatory-meditated neurodegenerative disorders as well. In experimental autoimmune encephalomyelitis (EAE), an animal model for multiple sclerosis, CNI-1493 given prior to the onset of clinical symptoms was able to suppress the disease and ameliorate symptoms when given in the chronic phase (10). Transgenic superoxide dismutase 1 (SOD1) mutant mice, a model for amyotrophic lateral sclerosis, showed increased survival and decreased motor neuron degeneration after treatment with CNI-1493 (11). In the central nervous system, CNI-1493 was also able to inhibit endogenous synthesis of nitric oxide (NO) and inflammatory cytokines and thus protect against development of cerebral infarction (12) as well as formalin-induced hyperalgesia(13).

More recently, a beneficial effect in Parkinson's disease has been shown. Neuronal cell death induced by stereotactic injection of α-synuclein protofibrils in the rat substantia nigra could be markedly attenuated by intraperitoneal injection of CNI-1493 (14). Our group has previously shown that the MAPK inhibitor CNI-1493 can ameliorate the pathophysiology in TgCRND8 mice, a murine AD model that overexpresses human amyloid precursor protein (APP). CNI-1493 not only suppressed development of Aβ plaques, but also improved cognitive function in these mice. As anticipated based on CNI-1493's suppressive effects on macrophages, treatment with CNI-1493 was accompanied by microglial deactivation (15).

In the present study, we set out to further elucidate the protective mechanism of CNI-1493 in AD. To date, the protective effect of CNI-1493 in preclinical AD models had remained speculative. On the one hand, CNI-1493 could attenuate reactive neuroinflammation elicited by Aβ aggregates. On the other hand, we have previously shown that CNI-1493 can reduce Aβ plaque formation *in vitro* and *in vivo*. To differentiate the compound's effects on these functions, we employed the CNI-1493 analogue Compound 1213 (C1213), which has a strong structural similarity to the parent molecule (lacking only four double bonds) but does not show antiinflammatory effects *in vitro*. This allowed us to tease out two possible mechanisms of CNI-1493's effects on AD symptomatology and elaborate on the contribution of both neuroinflammation and Aβ toxicity in this AD model. We discovered that, like CNI-1493, C1213 interacted with soluble and insoluble Aβ aggregates in cell-free systems. Moreover, it suppressed Aβ cytotoxicity *in vitro*. Finally, C1213 attenuated Aβ toxicity in a nematode model and reduced Aβ plaque burden and cognitive deficits in transgenic CRND8 mice. Taken together, our findings suggest that the effects of CNI-1493 are mainly driven by a reduction of Aβ cytotoxicity. Thus CNI-1493, a drug with proven safety in humans, is a viable candidate for novel therapeutic approaches to AD.

MATERIALS AND METHODS

Drug Preparation

CNI-1493 and C1213 were dissolved in dimethyl sulfoxide (DMSO; 100 mM) and kept at –20°C until use.

Amyloid β Preparation

Recombinant Aβ 1-42 peptide (Anaspec) aggregates were prepared as previously described (16), with slight modifications. For soluble aggregates, Aβ peptide (0.45 mg/mL) was dissolved in hexafluoroisopropanol and deionized water (ratio 4:6), sonicated for 5 min and incubated with a mini stir bar for 24 h at room temperature. The evaporated volume was reconstituted with deionized water and the solution was used for cell treatment. For insoluble aggregates, Aβ peptide was dissolved in hexafluoroisopropanol (HFIP), sonicated for 5 min and lyophilized. Prior to the experiment, the pellet was dissolved in phosphate-buffered saline (PBS; 0.45 mg/mL) and incubated at 36°C for 24 h.

Aggregation Assays

For A11, ELISA was conducted as previously described (15). Aβ1-42 oligomers (0.3 mg Aβ/mL H_2O) were diluted in coating buffer (50 ng/100µl, 0.1 M sodium bicarbonate, pH 9.6), and 100 µl of samples were added to 96-well high-binding microplates (Corning). Incubation lasted for 1 h at 37°C, followed by three washes using Tris-buffered saline (TBS), Tween 20 (0.01% Tween 20; TBS-T), and blocking for 2 h at 37°C with 10% bovine serum albumin (BSA) in TBS-T. All wells were washed three times with TBS-T and for 1 h at 37°C with 100 µl of anti-Aβ oligomer A11 antibody (1:2,000 in 5% nonfat milk/TBS-T; kindly provided by R. Kayed.) After being washed three times with PBS-T, the plates were incubated for 1 h at 37°C in 100 µl horseradish peroxidase–conjugated anti-rabbit IgG (diluted 1:10,000 in 5% nonfat milk/TBS-T; Promega). After a final three washes with TBS-T, the plates were developed using 3,3′,5,5′-tetramethylbenzidine (KP); 100 µl 1M HCl was used to stop the color reaction. Plates were immediately read at 450 nm.

Thioflavin T Assay

Thioflavin T (ThT; Sigma Aldrich) was dissolved in 50 mM glycine buffer (pH 8.5) to generate a working reagent; 90 µl of the working solution (5 µM ThT) was pipetted in a black 96-well plate (Corning) and 10 µl of the Aβ fibril solution was added to each well. Fluorescence measurement was

conducted in a plate reader (Tecan) at excitation 440 nm and emission 490 nm.

Native Gel Electrophoresis

Soluble Aβ aggregate was dissolved in native sample buffer. A volume containing 500 ng Aβ peptide was loaded in each well and separated under native nonreducing conditions. Western blot was conducted at 100 for 30 min using a 0.2 µm nitrocellulose membrane. After transfer, the membrane was heated in a microwave for 6 min in Mg- and Ca-free PBS and probed with 6E10 anti-Aβ antibody (BioLegend).

Cell Lines

BV-2 cells were derived from raf/myc-immortalized murine neonatal microglia and are the most frequently used substitute for primary microglia (17). RAW 264.7 is a macrophage-like cell line derived from tumors induced in male BALB/c mice by the Abelson murine leukemia virus. Wild-type APP overexpressing transgenic SH-SY5Y cells were kindly provided by Philippe Marambaud, PhD (18).

In Vivo and *Ex Vivo* Experiments

All animal experiments were conducted in strict compliance with the Guide for the Care and Use of Laboratory Animals, Institute for Laboratory Animal Research, Division on Earth and Life Studies (19), European Directive no. 86/609, and the guidelines of the local institutional animal care and use committee.

Primary cortical cell cultures. For mouse cortical cultures, E 13.5 Swiss mouse embryos were used (Janvier Breeding Center, France). The dissected tissue pieces were processed according to previously described protocols for mesencephalic cultures (20,21). Briefly, after mechanical dissociation in modified L15 medium (22) with no enzymatic treatment, the cells in suspension were plated at a density of 1.5–2.0 × 10^5 cells/cm^2 in polyethylenimine (1 mg/mL; Sigma Aldrich) precoated culture plates (24 wells). The cells were then allowed to mature and differentiate in neurobasal A-medium supplemented with B27 supplement and 1% penicillin/streptomycin.

In some experiments, cytarabine (2 µM) was added to the medium at 1–2 d *in vitro* (DIV) after plating to inhibit proliferation of nonneuronal cells (astrocytes, microglia).

Highly enriched microglial cultures from mice ventral mesencephalon. Almost pure microglial cultures were obtained using a technique of high-yield isolation of microglia by mild trypsinization (23). Briefly, neuronal/glial mesencephalic cultures were prepared as described previously, except for the culture medium, which was Dulbecco's modified Eagle medium/F-12 nutrient mixture (DMEM/F12; Invitrogen) supplemented with 10% fetal calf serum (FCS). After 14 DIV, the cultures were washed for 1 min with DMEM-F12 to eliminate serum and then incubated with a trypsin-ethylenediaminetetraacetic acid (EDTA) solution (0.25% trypsin, 1 mM EDTA in Hank's Balanced Salt Solution (HBSS; Invitrogen) diluted 1:4 in DMEM/F12 for 30 min to 1 h at 37°C until the upper layer (mainly constituted in neurons/astrocytes) was detached. The medium containing the layer of detached cells was aspirated, and the highly enriched microglial cell population (99% of pure microglial cells) that remained attached to the bottom of the well was exposed to 500 µl of DMEM/F12 with 10% FCS to allow trypsin inactivation.

Proliferation and toxicity assays. Cells were allowed to incubate for 1 h at 37°C with 3-(4,5-dimethylthiazol-2-yl)-2, 5-diphenyltetrazolium bromide (MTT) (500 µg/mL in culture medium; Sigma Aldrich). Following this incubation, the solution was removed and cells were lysed at room temperature for 30 min in DMSO. Absorbance was measured at 570 nm using a plate reader. Percentage of surviving cells was calculated in respect to untreated cells.

Lactate dehydrogenase (LDH) cytotoxicity assay (Roche) was performed according to the manufacturer's protocol. Absorbance was measured at 490 nm using a plate reader. For negative control, cells were lysed with 1% Triton 100 beforehand. Percentage of LDH release was calculated in respect to the negative control.

Cytokine ELISA assay. TNF, IL-6 and IL-10 concentrations in cell culture medium or blood serum were determined by ELISA. ELISA kits (R&D Systems) were used according to the manufacturer's protocol. SuperBlock® (Thermo Fisher Scientific) was used for blocking and 3,3',5,5'-tetramethylbenzidin (TMB; Calbiochem, Darmstadt, Germany) for development. The reaction was stopped with 2N H_2SO_4 and absorption was measured at 450 nm using a plate reader. Cytokine concentrations were calculated with respect to a standard curve.

Western blot analysis. Protein isolation from cell cultures was performed 15 min after lipopolysaccharide (LPS) stimulation. Cells and proteins were placed on ice immediately. Cells were washed with PBS and lysed with mammalian protein extraction reagent (M-PER; Thermo Fisher Scientific) containing protease inhibitor cocktail and phosphatase inhibitor (Roche). Brains were homogenized in tissue protein extraction reagent (T-PER; Thermo Fisher Scientific) containing protease inhibitor cocktail and phosphatase inhibitor (Roche). Proteins were isolated according to the manufacturer's protocol. Protein concentration was measured with a spectrophotometer (NanoDrop; Thermo Fisher Scientific). Samples (10 µg protein per lane) were loaded onto precast NuPAGE Novex 4-12% Bis-Tris gels using the Novex electrophoresis system (Invitrogen). Subsequently, proteins were transferred onto nitrocellulose membranes (Invitrogen) using the XCell II blot (Invitrogen). Membrane-bound protein was visualized using MemCode reversible protein staining kit (Perbio). Membranes were blocked for 1 h at room temperature or overnight at 4°C with blocking buffer (5% BSA in TBS with 0.1% Tween 20). Primary antibodies were diluted in blocking buffer as follows: anti-phospho-p44/42 MAPK (Thr202/Tyr204) rabbit mAb (Cell Signaling, distributed

by New England Biolabs) 1:2,000, anti-phospho-p38 MAPK (Thr180/Tyr182) rabbit mAb (Cell Signaling) 1:1,000, anti-phospho-SAPK/JNK (Thr183/Tyr185) rabbit mAb (Cell Signaling) 1:1,000, anti-GAPDH mouse mAb (Novus Biologicals, distributed by Acris) 1:20,000. Membranes were incubated with primary antibody for 1 h and then washed three times for 15 min with 0.1% TBS-Tween. Secondary antibodies were diluted in 1 × Roti Block (Roth) as follows: anti-rabbit IgG HRP linked antibody (Cell Signaling) 1:4,000, anti-mouse IgG HRP linked antibody (Thermo Fisher Scientific) 1:25,000. Membranes were washed three times for 15 min with TBS + 0.1% Tween and incubated for 5 min in SuperSignal West Dura Extended Duration Substrate working solution (Thermo Fisher Scientific). Afterward, the membranes were exposed to autoradiographic film (CL-Xposure Film, Thermo Fisher Scientific).

Drug treatment of TgCRND8 mice. Nine female and nine male TgCRND8 mice (hemizygously overexpressing a double-mutant human *APP695* transgene [hAP*P* + /–] containing the "Swedish" [KM670/671NL] and "Indiana" [V717F] mutations under the control of hamster prion protein promoter) (24) were housed in groups of three to four animals from postnatal d 30 (P30) until P150. To control for the parental genotype, each litter was equally divided into treatment and control groups. Three-month-old mice received biweekly intraperitoneal injections of either 100 µl containing 200 µg C1213 (dose, 8 mg/kg; 0.043% v/v diluted in 0.9% NaCl) (n = 5 per gender) or 100 µl DMSO (0.043% v/v diluted in 0.9% NaCl as control treatment) (n = 4 per gender) for 8 wks. Subsequently, mice were subjected to behavioral phenotyping. At the end of the experimental period, animals were euthanized and the brain hemispheres were separated along the midline. One hemisphere was fixed in 4% buffered formaldehyde for 24 h, followed by dehydration and paraffin embedding. The other hemisphere was immediately snap-frozen in liquid nitrogen and kept at –80°C until use.

Behavioral testing of TgCRND8 mice. To investigate the treatment efficacy of C1213 on visuospatial learning and memory in TgCRND8 mice, we performed the object location test (OLT). The OLT is based on the spontaneous tendency of rodents to explore an object moved to a new location more often than an object located at a familiar position (25). Animals are exposed to two identical objects in an experimental apparatus and, after a delay, reexposed to the same two objects, one of which has been moved to a new location. Animals that remember the previous exposure spontaneously show a bias, ie, higher exploration times, toward the object in the new position.

For analysis of OLT, cumulative exploration times with respect to each object in the training and test trial were recorded for each mouse. In addition, a recognition index, ie, time spent exploring the object in the novel location versus total time spent exploring both objects in the test trial, was calculated for each mouse. A recognition index of 50% was expected under chance conditions, while higher percentages were interpreted as bias to an object. Analysis of the recognition index was less susceptible to individual variability and provided a measure of the extent of discrimination between novel and sample objects. Mice with cumulative exploration times of less than 2 s were excluded from OLT due to reduced exploratory behavior.

Animals had free access to tap water, were fed ad libitum and were kept under standard conditions. TgCRND8 was assigned randomly to the experimental groups. The investigator was blinded to the treatment assignment. Behavioral testing was conducted during the light period between 08:00–18:00 h. Behavioral data for both genders were pooled after observing no gender differences in behavioral responses to the OLT. Three animals passed away before entering behavioral experimentation. Therefore, a total of 15 TgCRND8 mice completed behavioral testing.

Plaque morphometry in TgCRND8 mice. For morphometric analysis, a Nikon 80i microscope with an integrated CFI ocular lens (10 × magnification) equipped with a CFI PLAN FLUOR objective (20 × magnification, numerical aperture 0.5), a color digital camera (3/4" chip, 36-bit color, DV-20, MicroBrightField), and MicroBrightField software were used. Aβ plaques (1:100, 6F/3D, DAKO) were visualized and stereologically quantified in 10 sections (with 100 µm distance between sections) per staining and animal at 200 × magnification. Aβ plaque volume (ie, percentage of cerebral volume covered by deposits) and Aβ plaque number (n/mm^2) were calculated in an unbiased manner by area fraction fractionator and fractionator (counting frame and grid size, each 500 × 500 µm), respectively.

Nematode paralysis assay. Caenorhabditis elegans strains N2, CL2006 (dvIs2 [pCL12(unc-54/human Aβ peptide 1-42 minigene) + pRF4]) and CL4176 (smg-1(cc546ts) I; dvIs27 [myo-3/ Aβ minigene + rol-6(su1006) marker gene]) were kindly provided by the Caenorhabditis Genetic Center (CGC), which is funded by the National Institutes of Health Office of Research Infrastructure Programs (P40 OD010440). Worms were maintained on solid media spotted with Escherichia coli OP50 (provided by CGC). Effects of drugs were assessed using the CL4176 strain in a paralysis assay (26). Briefly, synchronized worm colonies were obtained through synchronous egg lay; 48 h after egg lay, the temperature was raised from 16 to 25°C and paralysis was assessed repeatedly by a blinded observer between 20 and 30 h after temperature increase. Each condition was measured in triplicate. Representative results from three independent experiments are shown. Thioflavin S (Sigma Aldrich) staining of intramuscular Aβ plaques was conducted and imaged as previously described (27).

Statistics

Data were analyzed using analysis of variance (ANOVA) for several

independent variables or Student *t* test for single independent variables. A significance level (*) of 0.05 was selected, and two-sided tests were performed.

RESULTS

The protective effect of CNI-1493 in AD preclinical models has been attributed to its multiple functions as an antiinflammatory agent and an inhibitor of amyloid plaque formation *in vitro* and *in vivo* (15). In the present study, we raised the question of whether both activities are required. To this end, we developed an analogue of CNI-1493 that lacks the antiinflammatory properties while preserving inhibition of Aβ oligomer and plaque formation. We screened a focused library around the CNI-1493 scaffold and identified C1213 as a lead candidate (see Figure 1 for chemical structures).

Despite minor differences in molecular structure, C1213 showed an improved profile with regard to *in vitro* cell proliferation and toxicity. *In vitro* cytotoxicity screening was performed on primary neuronal and microglial cell cultures using MTT and LDH assays, respectively. CNI-1493 completely inhibited cell proliferation at concentrations above 20 μM in microglia (Figure 2A) and neurons (Figure 2C). These reductions in cell proliferation were accompanied by enhanced LDH secretion at concentrations of CNI-1493 above 20 μM (Figures 2B and D). These effects on cell proliferation and LDH secretion were significantly attenuated with C1213 ($p < 0.01$).

Next we assessed the antiinflammatory properties of C1213. While CNI-1493 is a potent MAPK inhibitor, C1213 did not display MAPK inhibitor activity. BV-2 microglial cell line (Figure 3A) and primary murine microglia (Figure 3B) were pretreated for 1 h with CNI-1493 and C1213, respectively, prior to stimulation with LPS. After 15 min, cells were lysed and phosphorylation of the three MAPK p38, ERK and JNK was assessed using Western blot. CNI-1493 had a dose-dependent inhibitory effect on all three MAPK (Figures 3A and B). Strikingly, C1213 lacked MAPK inhibitor activity at concentrations up to 20 μM. In line with these findings, C1213 failed to attenuate LPS-induced release of the canonical proinflammatory cytokines TNF and IL-6 or the antiinflammatory IL-10 at concentrations up to 30 μM (Figures 3C–E). Thus, in contrast to CNI-1493, C1213 lacked MAPK inhibitor activity.

We have previously reported that CNI-1493 affects APP metabolism and reduces Aβ deposition *in vivo* (15). Furthermore, we have shown that CNI-1493 directly interacts with Aβ *in vitro* (28). In the next set of experiments, we studied the effects of C1213 on Aβ1-42 in a cell-free system. To this end, an Aβ1-42 oligomer preparation was incubated with increasing concentrations of CNI-1493 or C1213 (molar ratios 0.1:1, 1:1 and 10:1 C1213 to Aβ) at 36°C for 3 h. After incubation, the Aβ compound solution was separated on a native gel and Western blot was probed with 6E10 anti-Aβ antibody. Interestingly, CNI-1493 and C1213 led to a reduction of the Aβ signal that was absent in vehicle-treated samples (Figure 4A). Similarly, 3 h incubation with CNI-1493 and C1213 reduced A11 antibody reactivity of Aβ1-42 oligomer preparations as measured by ELISA (Figure 4B; Veh versus CNI: $p < 0.001$; Veh versus C1213: $p < 0.001$; CNI versus 1213: $p > 0.05$). Likewise, CNI-1493 and C1213 attenuated thioflavin T fluorescence after 3 h incubation of Aβ1-42 fibrils at 36°C (Figure 4C; Veh versus CNI: $p < 0.001$; Veh versus C1213: $p < 0.001$; CNI versus 1213: $p > 0.05$; Veh versus control: $p > 0.05$). Finally, CNI-1493 and C1213 were equally effective in attenuating the effect of Aβ1-42 on the proliferation of primary microglia assessed by MTT assay (Figure 4D; Veh versus CNI: $p < 0.001$; Veh versus C1213: $p < 0.001$). We have previously shown that the protective effect of CNI-1493 *in vitro* is solely driven by interaction with Aβ aggregates, as CNI-1493 alone

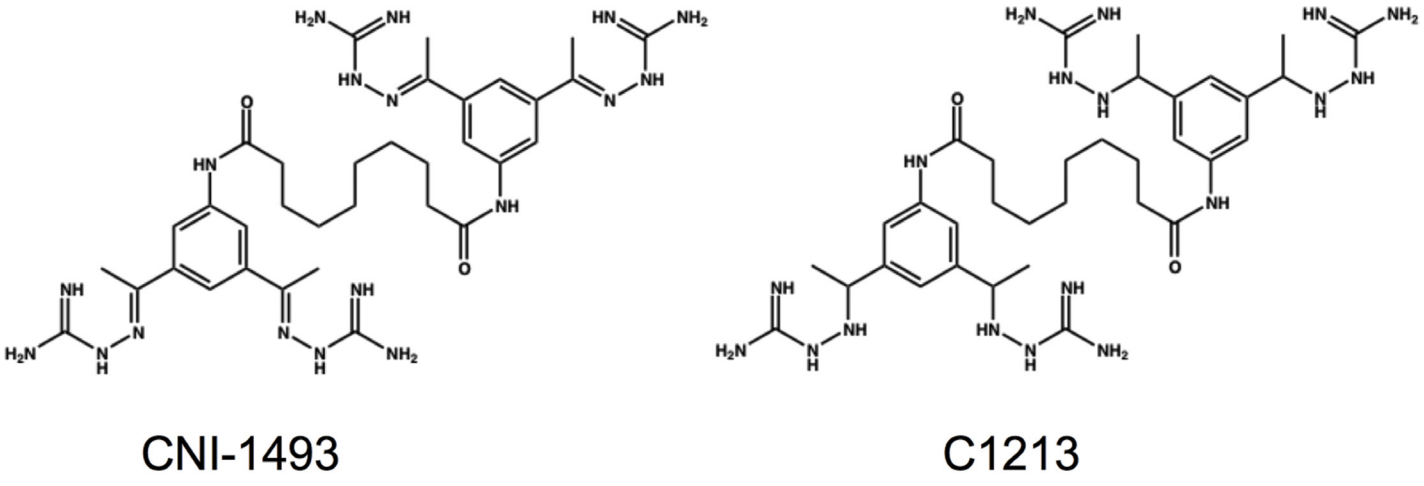

Figure 1. Molecular structures of CNI-1493 and Compound-1213.

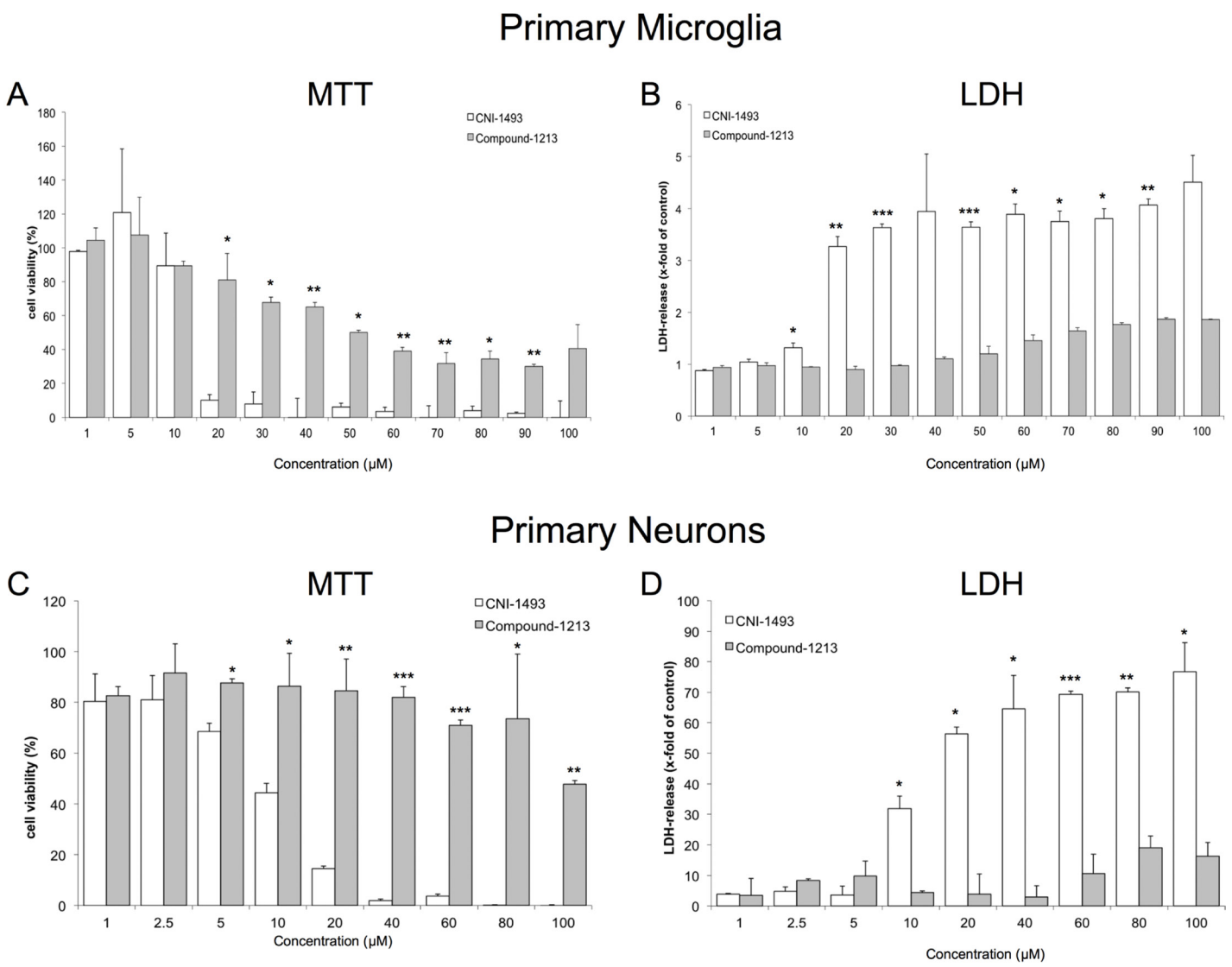

Figure 2. C1213 *in vitro* is considerably less toxic than CNI-1493. Primary microglia (A + B) and primary neurons (C + D) were treated with the indicated concentrations of CNI-1493 or Compound-1213 for 24 h. Cell proliferation (A + C) and cell death (B + D) were analyzed by MTT and LDH assay, respectively. * $P < 0.05$, ** $P < 0.01$, *** $P < 0.001$.

had no protective effect on apoptotic cells and nonaggregated Aβ had no adverse effects of microglial proliferation (28). Therefore, these findings suggest that C1213 interacts with Aβ1-42 oligomers and fibrils at concentrations comparable to CNI-1493. Also, this interaction reduced the inhibitory effect of Aβ1-42 aggregates on microglial proliferation.

Next, we wondered if C1213 would attenuate *in vivo* cytotoxicity of Aβ1-42 aggregates. The effects of Aβ1-42 in mammals are presumably mediated through Aβ-induced inflammation as well as direct cytotoxicity. We sought to test our drugs in the latter form of Aβ toxicity. Such toxicity might be driven by intracellular Aβ aggregates. The potential mechanism of action is intracellular accumulation and disruption of cellular function from within (29). Notably, selective accumulation of intracellular Aβ in reelin-positive neurons of the entorhinal cortex was recently suggested as an early hallmark of AD (30). To test whether Aβ can accumulate intracellularly, we extracted the cytosolic fraction of WT and APP overexpressing transgenic SH-SY5Y (APPtg SH-SY5Y) and probed it with the 4G8 anti-Aβ antibody. In contrast to WT cells, APPtg SH-SY5Y showed a band consistent with cytosolic Aβ (Figure 5A). Intracellular Aβ accumulation could occur in a similar fashion in AD mouse models overexpressing mutants of APP. Since the distinction between the impacts of intracellular and extracellular Aβ toxicity is challenging in mice, we tested CNI-1493 and C1213

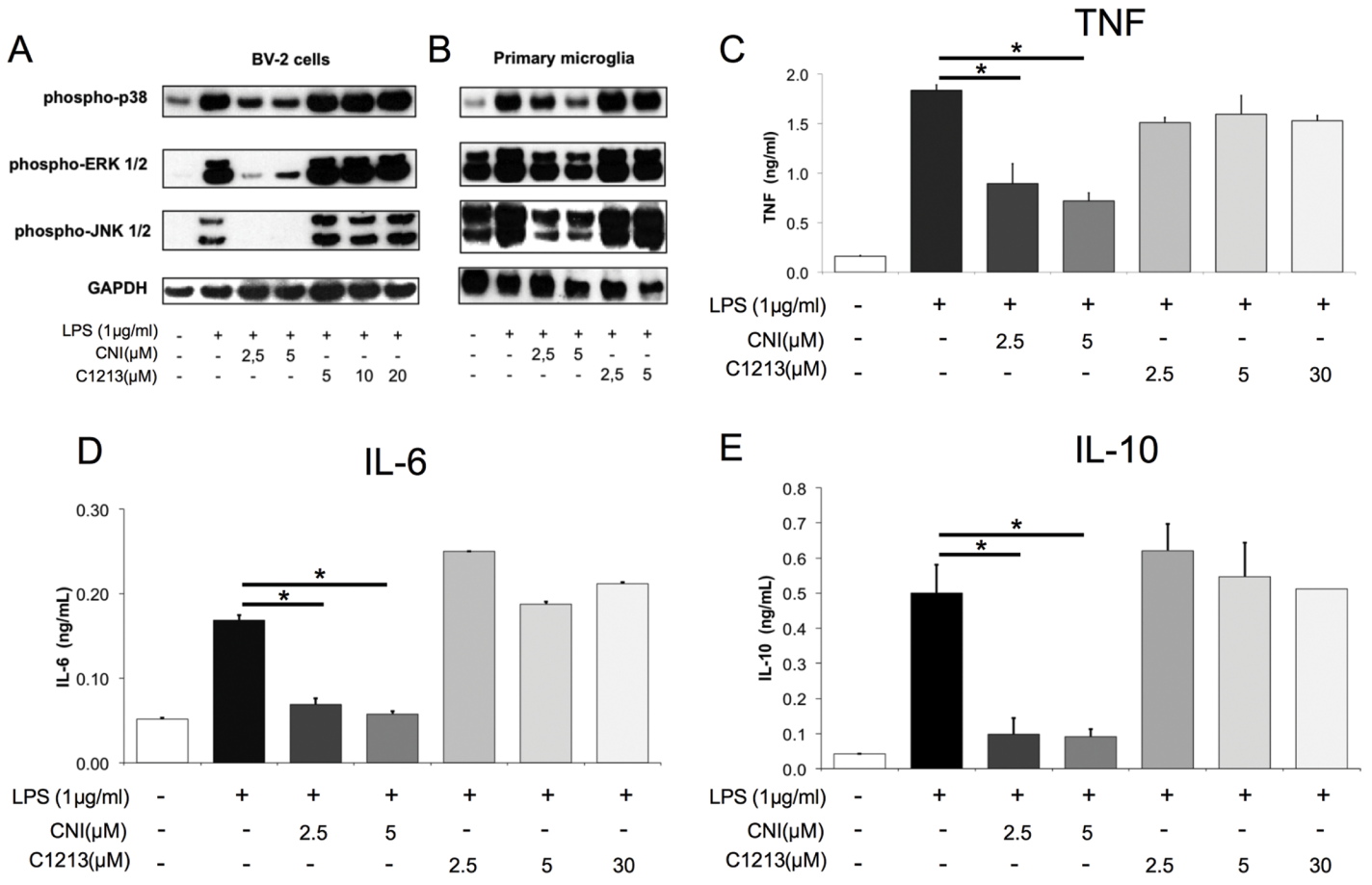

Figure 3. C1213 does not inhibit phosphorylation of MAP-kinases or cytokine secretion in primary microglia. (A-B) MAP-kinase western blot: (A) BV-2 cells or (B) primary microglia were treated with the indicated concentrations of CNI-1493 or C1213 1 h prior to LPS treatment (1µg/mL). Cells were lysed 15 min after LPS treatment and western blot analysis against phospho-p38, phospho-ERK 1/2, phospho-JNK 1/2 and GAPDH was performed. (C-D) Cytokine ELISA: Primary microglia were treated with CNI-1493 (2.5 and 5 µM) or C1213 (2.5, 5 and 30 µM) 1 h prior to LPS treatment (1µg/ml). The following cytokine concentrations in the media were determined via ELISA analysis: (C) TNF 1 h, (D) IL-6 2 h, and (E) IL-10 7 h after LPS treatment. * p<0.05.

in a Caenorhabditis elegans model of intramuscular Aβ accumulation (26,31). In this model, intramuscular overexpression of Aβ1-42 (Figure 5B) leads to formation of plaques and acute paralysis of the animals. Thioflavin S staining of such plaques is limited to body wall muscles (Figure 5C). Aβ overexpression was induced in worms placed on agar containing CNI-1493, C1213 or Veh, and the number of paralyzed animals was counted over time. We observed attenuated paralysis in worms on agar containing CNI-1493 or C1213 (Figure 5D; Veh versus CNI: $p < 0.001$; Veh versus C1213: $p < 0.01$; CNI versus C1213: $p > 0.05$). Thus, C1213 can attenuate intracellular Aβ toxicity.

Finally, we tested the effects of C1213 in the CRND8 AD mouse model. We have previously reported attenuated cognitive deficits and neuroinflammation in this mouse strain following CNI-1493 treatment (15). C1213 improved performance in the OLT (Figures 6A–C) with C1213-treated mice displaying the preference (Figure 6B; $p < 0.001$) and recognition index (Figure 6C; $p < 0.01$) of the moved object in the test trial. Moreover, C1213 reduced the Aβ plaque volume (Figure 6D; $p < 0.05$) without affecting plaque numbers (Figure 6E; $p > 0.05$). Thus, like its parent compound CNI-1493, C1213 improves behavioral deficits and the immunohistopathology in CRND8 AD transgenic mice.

DISCUSSION

After several decades of Alzheimer's disease research, the pathophysiological mechanisms remain elusive. To address this issue, several hypotheses have been proposed as drivers of the pathology, including the cholinergic, amyloid-β, tau and inflammation hypotheses. Unfortunately, all therapies targeting a single pathway within these hypotheses have failed so far.

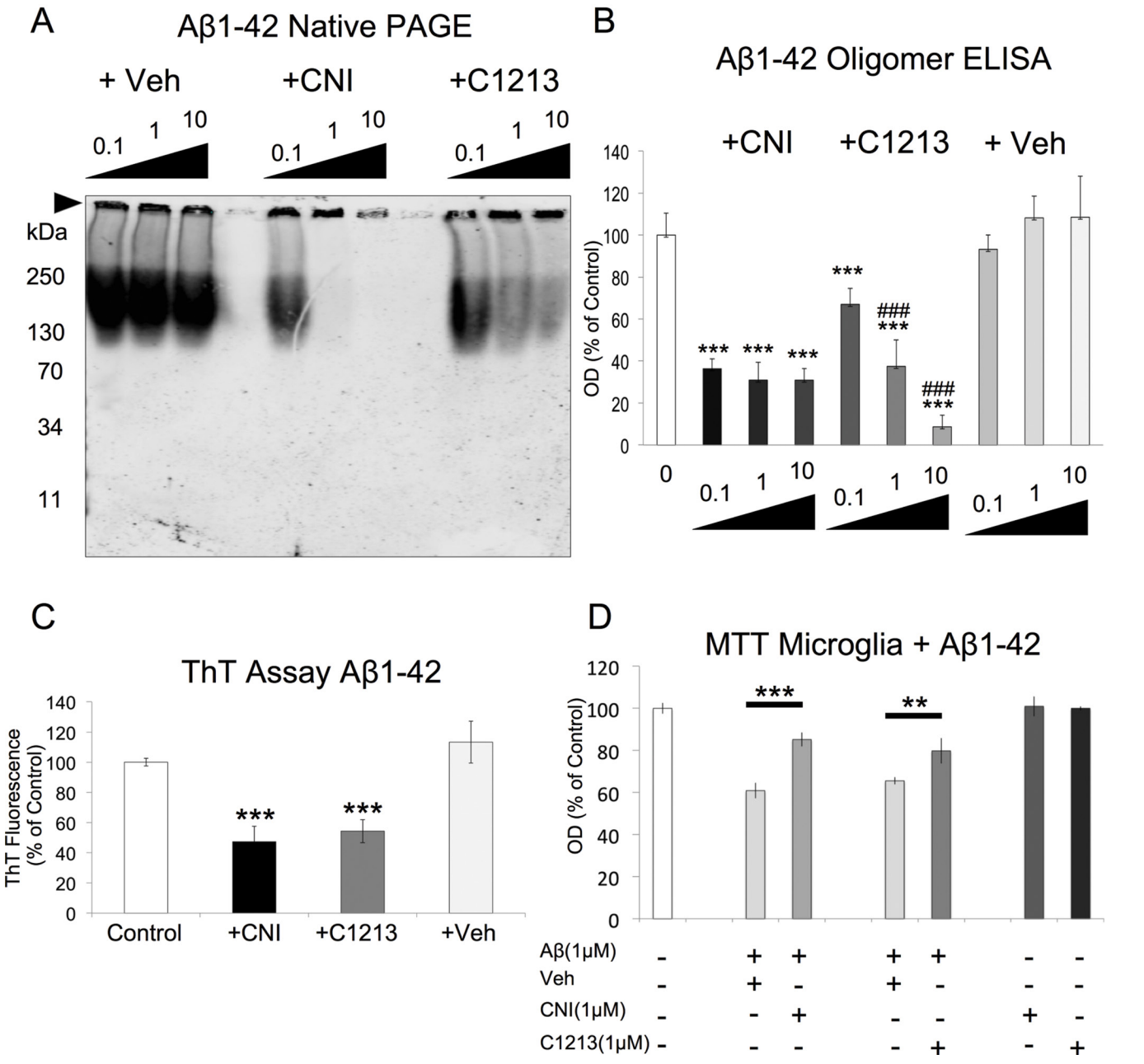

Figure 4. C1213 and CNI-1493 change Aβ 1-42 aggregation *in vitro*. Soluble Aβ 1-42 aggregates were incubated for 3 h with different ratios of compound:Aβ (0.1:1, 1:1, 10:1). (A) Native gel electrophoresis and Western blot (6E10 anti-Aβ antibody) show reduction in soluble Aβ aggregates entering the running gel, with Aβ remaining in the stacking gel (arrowhead). (B) A11 oligomer-specific ELISA shows reduction in immunoreactivity following incubation with CNI-1493 and C1213. (C) CNI-1493 and C1213 reduce the Thioflavin T signal of insoluble Aβ 1-42 aggregates. (D) MTT assay of primary microglia treated for 48 h with soluble Aβ 1-42 aggregates incubated for 3 h with vehicle, CNI-1493 or C1213. Incubation of Aβ 1-42 aggregates with CNI-1493 or C1213 attenuates Aβ-induced reduction of the MTT signal. *** $P < 0.001$ Veh vs. Compound; ### $P < 0.001$ for dose-dependent reduction in signal.

A possible explanation for these failures is that either each single-tested hypothesis is wrong or a combination of factors is at play.

In the present study, we explore the role of the multitarget compound CNI-1493 as a compound simultaneously targeting several aspects of Alzheimer's disease. While the antiinflammatory properties of the macrophage deactivator CNI-1493 are firmly established in rodents and humans,

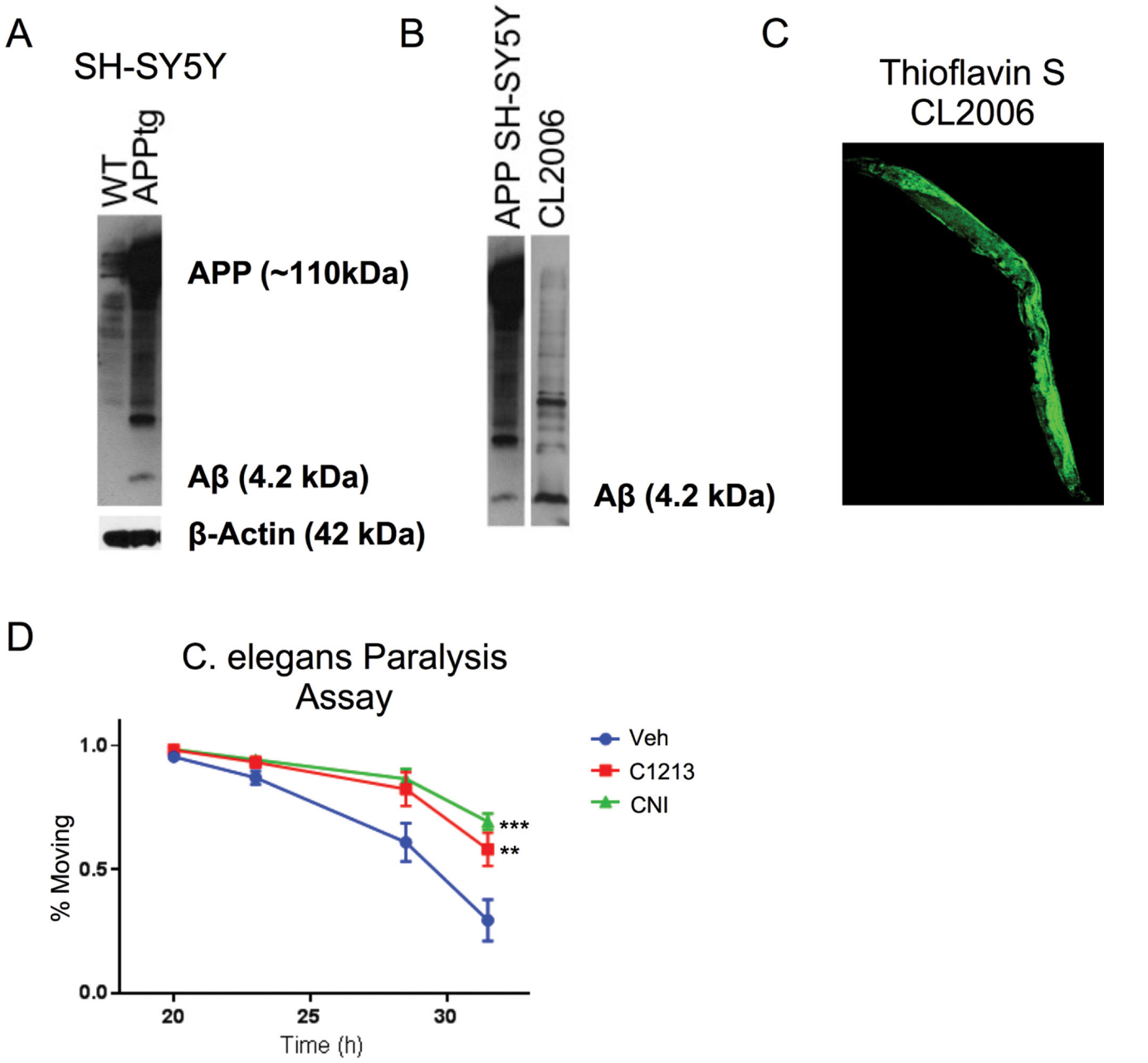

Figure 5. C1213 and CNI-1493 attenuate in vivo Aβ 1-42 toxicity in *C. elegans*. (A) Western blot of the cytosolic fraction of amyloid precursor protein overexpressing SH-SY5Y shows a band consistent with cytosolic Aβ that is not present in wild-type cells. (B) Western blot of the CL2006 *C. elegans* model of muscular Aβ 1-42 overexpression and paralysis shows Aβ reactivity in worm lysates. (C) CL2006 Aβ 1-42 overexpressing worms were stained with Thioflavin S and visualized using confocal microscopy. (D) CNI-1493 and C1213 attenuate Aβ-induced paralysis in the CL4176 C. elegans model of muscular Aβ 1-42 overexpression and paralysis. ** $P < 0.01$ Veh vs. Compound; *** $P < 0.001$ Veh vs. Compound.

the antiamyloidogenic properties have been less appreciated. Here, we unequivocally establish the antiamyloidogenic properties of CNI-1493 utilizing a multimodal approach. First, we generated C1213 as a novel analogue of CNI-1493 lacking antiinflammatory properties. *In vitro*, we show that C1213 does not inhibit MAP kinase phosphorylation and cytokine secretion in the BV-2 microglial cell line and primary microglia. Notably, C1213 and CNI-1493 show similar effects on Aβ aggregation in a cell-free system and on Aβ toxicity *in vitro*. Furthermore, both compounds

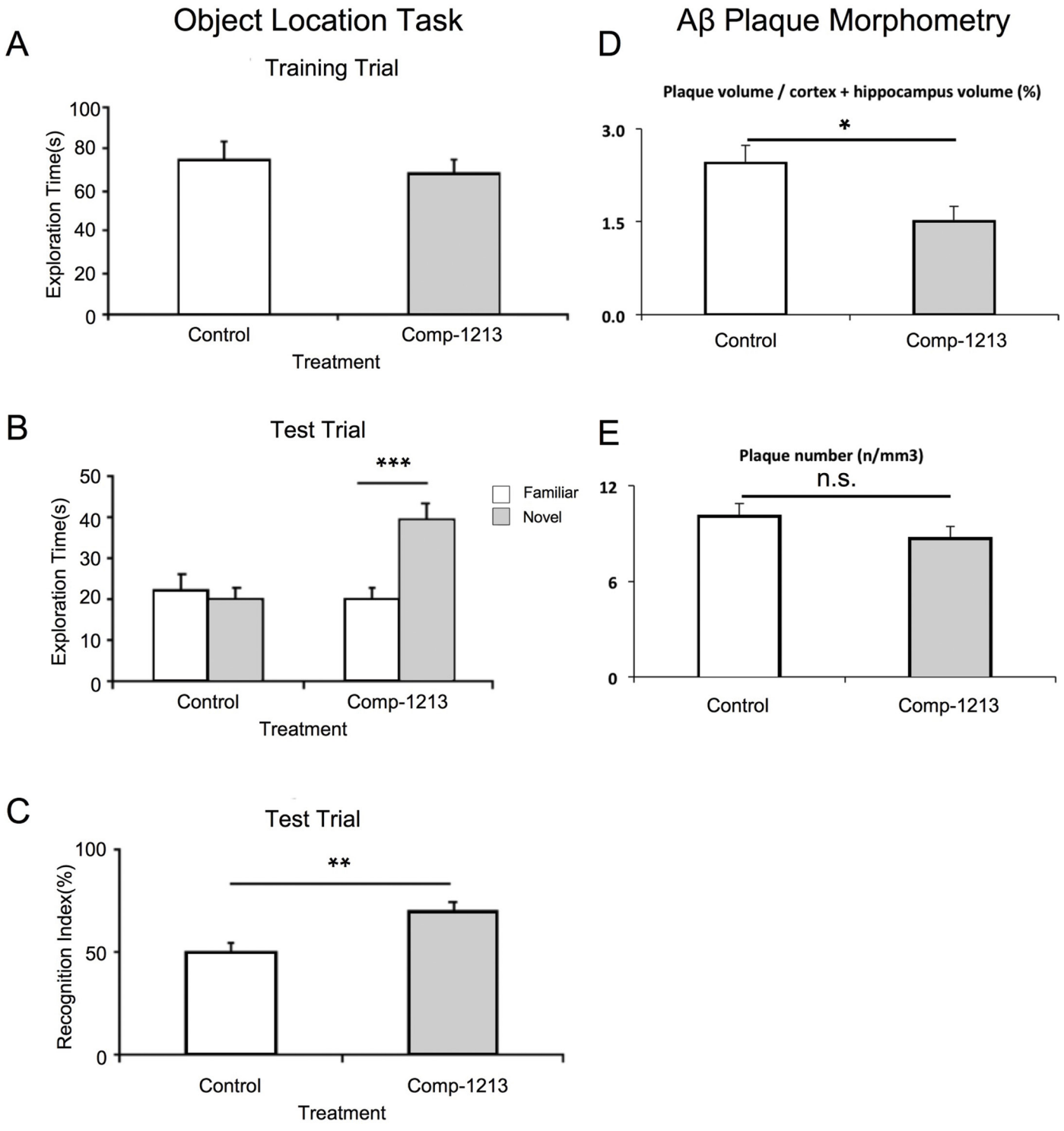

Figure 6. C1213 attenuates Aβ-induced cognitive deficits and reduces Aβ plaque volume in CRND8 transgenic mice. (A–C) An object location task was performed with Veh- and C1213-treated CRND8 mice. (A) Both treatment groups showed equivalent object exploration times in the test trial. (B) C1213-treated mice displayed preferential examination of the object moved to a novel location and (C) a significantly enhanced recognition index. (D–E) Immunohistochemical analysis of Aβ plaques in CRND8 mice. (D) Treatment with C1213 significantly reduced Aβ plaque volume while (E) plaque number remained unchanged. * $P < 0.05$; ** $P < 0.01$; *** $P < 0.001$. n.s., not significant.

have equivalent protective effects in a nematode model of intracellular Aβ toxicity. This is noteworthy, since in the nematode model used in this study, Aβ toxicity only occurs intracellularly and contribution by immune cells seems unlikely. Finally, we show that C1213 reduces Aβ plaque volume and enhances cognition in the CRND8 mouse model of Alzheimer's disease. Our data therefore strongly suggest that the beneficial effects of C1213 and CNI-1493 occur through direct interaction with Aβ aggregates. Thus, CNI-1493 could serve as a lead for development of a novel class of drugs targeting multiple disease pathways in complex disorders leading to neurodegeneration. Our approach is in line with the notion of rational pharmacology targeting protein interaction networks instead of single proteins (32).

CNI-1493 was initially developed for inhibition of nitric oxide synthesis by activated macrophages (1). Interestingly, it was found to inhibit inflammatory responses (3) through p38 MAP kinase inhibition and suppression of TNF (3,5) We previously described protective effects of CNI-1493 in the CRND8 mouse model of Alzheimer's disease, showing attenuated inflammation and reduced amyloidosis in animals treated with the drug. However, at that point we were unable to distinguish between direct effects of CNI-1493 and indirect effects through modulation of microglial activation. The newly synthesized analogue C1213 showed that CNI-1493 indeed acted *in vivo* through direct interaction with Aβ aggregates. The multitarget properties of CNI-1493 were further corroborated through differential effects of CNI-1493 and C1213 on the CRND8 mouse model. While CNI-1493 massively reduced Aβ plaque number and volume (14), the administration of C1213 merely reduced plaque volume at a statistically significant level. This difference suggests that microglial modulation through CNI-1493 is required for reduction of the plaque number. However, as previously suggested Aβ plaques do not correlate with the progression of Alzheimer's Disease pathology (33). Thus, our results suggest that the marked improvement of cognition in C1213-treated CRND8 mice results from interaction with oligomeric Aβ aggregates such as those recognized by the oligomer specific antibody A11 (16).

The link between inflammation and neurodegeneration remains controversial. We and others have shown that antiinflammatory intervention is promising in rodents. Moreover, epidemiological data suggested reduced incidence of Alzheimer's disease in patients taking nonsteroidal antiinflammatory drugs (NSAIDs) (34). However, a preventive clinical trial using NSAIDs failed to show statistical significance and was halted over safety considerations associated with preventive trials (35). NSAID intake reducing Alzheimer's disease incidence in human patients could also suggest that an increased inflammatory state in these patients due to the underlying disease might be protective against neurodegeneration. Indeed, some authors have argued that neurodegeneration is caused by an immunosuppressed state (36). This line of thinking also explains why enhancing immunity by blockading immune checkpoints can be beneficial in a rodent model of Alzheimer's disease (37). However, such therapies also promote autoimmunity. Several authors have uncovered mechanisms by which autoimmunity could cause neurodegeneration in humans (38,39). Additionally, enhanced anti-Aβ immunity through passive immunization with monoclonal anti-Aβ antibodies failed to improve cognitive symptoms (40) while potentially causing life-threatening meningoencephalitis. While acute immune activation and inflammation is beneficial for tissue maintenance and host defense, in chronic unresolving inflammation, negative aspects of immune activation called immunopathology may lead to structural damage and brain dysfunction (41). Finally, given that two genetic risk variants for Alzheimer's disease, CD33 (42) and TREM2 (43), disrupt microglial function, we argue that inhibitory immunomodulation of the innate immune system is a promising approach for the treatment of this disorder.

Due to the presence of Aβ plaques, Alzheimer's disease is considered a form of brain amyloidosis. Amyloidoses constitute a heterogeneous class of hereditary, chronic inflammatory or malignant diseases (44). Despite an urgent clinical need posed by amyloidoses, the available treatment options are mainly symptomatic. Novel and experimental causative therapies comprise proteasome inhibitors (45), immune modulators (46) or knockdown of the disease-causing protein (47). We have shown efficacy of CNI-1493 in reducing Aβ plaque load and driving Aβ uptake in microglia. Also, we and others show a protective role of CNI-1493 in 1-methyl-4-phenyl-1,2,3,6-tetrahydropyridine (48) and α-synuclein-driven (14) rodent models of Parkinson's disease. Thus, CNI-1493 as a compound with an immunomodulatory component and direct interaction with amyloid plaques offers a promising addition to this growing group of therapeutics.

CONCLUSION

Taken together, we have established *in vivo* and *in vitro* anti-amyloid activity in CNI-1493, a drug with a well-documented antiinflammatory profile. CNI-1493 is a multitarget drug with proven safety in humans. Therefore, it represents a promising agent for the treatment of complex diseases characterized by aberrant protein aggregation and inflammation, including but not limited to Alzheimer's disease.

ACKNOWLEDGMENTS

The authors are grateful to Sonya VanPatten PhD (Northwell Health, Manhasset, NY) for helpful comments on the manuscript.

DISCLOSURE

The authors declare that they have no competing interests as defined by *Molecular Medicine* or other interests that might be perceived to influence the results and discussion reported in this paper.

REFERENCES

1. Bianchi M, Ulrich P, Bloom O, *et al.* (1995) An inhibitor of macrophage arginine transport and nitric oxide production (CNI-1493) prevents acute inflammation and endotoxin lethality. *Mol. Med.* 1(3):254–66.
2. Dotan I, Rachmilewitz D, Schreiber S, et al. (2010) A randomised placebo-controlled multicentre trial of intravenous semapimod HCl for moderate to severe Crohn's disease. *Gut.* 59(6):760–66.
3. Bianchi M, Bloom O, Raabe T, et al. (1996) Suppression of proinflammatory cytokines in monocytes by a tetravalent guanylhydrazone. *J. Exp. Med.* 183(3):927–36.
4. Lowenberg M, Verhaar A, van den Blink B, et al. (2005) Specific inhibition of c-Raf activity by semapimod induces clinical remission in severe Crohn's disease. *J. Immunol.* 175(4):2293–2300.
5. Cohen PS, Schmidtmayerova H, Dennis J, et al. (1997) The critical role of p38 MAP kinase in T cell HIV-1 replication. *Mol. Med.* 3(5):339–46.
6. Granert C, Abdalla H, Lindquist L, et al. (2000) Suppression of macrophage activation with CNI-1493 increases survival in infant rats with systemic Haemophilus influenzae infection. *Infect. Immun.* 68(9):5329–34.
7. Specht S, Sarite SR, Hauber I, et al. (2008) The guanylhydrazone CNI-1493: an inhibitor with dual activity against malaria-inhibition of host cell pro-inflammatory cytokine release and parasitic deoxyhypusine synthase. *Parasitol. Res.* 102(6):1177–84.
8. Kemeny MM, Botchkina GI, Ochani M, Bianchi M, Urmacher C, Tracey KJ. (1998). The tetravalent guanylhydrazone CNI-1493 blocks the toxic effects of interleukin-2 without diminishing antitumor efficacy. *Proc. Natl. Acad. Sci. U.S.A.* 95(8):4561–66.
9. Atkins MB, Redman B, Mier J. (2001) A phase I study of CNI-1493, an inhibitor of cytokine release, in combination with high-dose interleukin-2 in patients with renal cancer and melanoma. *Clin. Cancer Res.* 7(3):486–92.
10. Martiney JA, Rajan AJ, Charles PC, et al. (1998) Prevention and treatment of experimental autoimmune encephalomyelitis by CNI-1493, a macrophage-deactivating agent. *J. Immunol.* 160(11):5588–95.
11. Dewil M, dela Cruz VF, Van Den Bosch L, Robberecht W. (2007) Inhibition of p38 mitogen activated protein kinase activation and mutant SOD1(G93A)-induced motor neuron death. *Neurobiol. Dis.* 26(2):332–41.
12. Meistrell ME 3rd, Botchkina GI, Wang H, et al. (1997) Tumor necrosis factor is a brain damaging cytokine in cerebral ischemia. *Shock.* 8(5):341–48.
13. Watkins LR, Martin D, Ulrich P, Tracey KJ, Maier SF. (1997) Evidence for the involvement of spinal cord glia in subcutaneous formalin induced hyperalgesia in the rat. *Pain.* 71(3):225–35.
14. Wilms H, Rosenstiel P, Romero-Ramos M, et al. (2009) Suppression of MAP kinases inhibits microglial activation and attenuates neuronal cell death induced by alpha-synuclein protofibrils. *Int. J. Immunopathol. Pharmacol.* 22(4):897–909.
15. Bacher M, Dodel R, Aljabari B, et al. (2008) CNI-1493 inhibits Abeta production, plaque formation, and cognitive deterioration in an animal model of Alzheimer's disease. *J. Exp. Med.* 205(7):1593–99.
16. Kayed R, Head E, Thompson JL, et al. (2003) Common structure of soluble amyloid oligomers implies common mechanism of pathogenesis. *Science.* 300(5618):486–89.
17. Henn A, Lund S, Hedtjarn M, Schrattenholz A, Porzgen P, Leist M. (2009) The suitability of BV2 cells as alternative model system for primary microglia cultures or for animal experiments examining brain inflammation. *ALTEX.* 26(2):83–94.
18. Chapuis J, Vingtdeux V, Campagne F, Davies P, Marambaud P. (2011) Growth arrest-specific 1 binds to and controls the maturation and processing of the amyloid-beta precursor protein. *Hum. Mol. Genet.* 20(10):2026–36.
19. Committee for the Update of the Guide for the Care and Use of Laboratory Animals, Institute for Laboratory Animal Research, Division on Earth and Life Studies. (2011) *Guide for the Care and Use of Laboratory Animals*, 8th ed. Washington, DC: National Academies Press. [accessed September 14, 2016]. Available at: https://oacu.oir.nih.gov/regulations-standards.
20. Michel PP, Agid Y. (1996) Chronic activation of the cyclic AMP signaling pathway promotes development and long-term survival of mesencephalic dopaminergic neurons. *J. Neurochem.* 67(4):1633–42.
21. Salthun-Lassalle B, Hirsch EC, Wolfart J, Ruberg M, Michel PP. (2004) Rescue of mesencephalic dopaminergic neurons in culture by low-level stimulation of voltage-gated sodium channels. *J. Neurosci.* 24(26):5922–30.
22. Knusel B, Michel PP, Schwaber JS, Hefti F. (1990) Selective and nonselective stimulation of central cholinergic and dopaminergic development in vitro by nerve growth factor, basic fibroblast growth factor, epidermal growth factor, insulin and the insulin-like growth factors I and II. *J. Neurosci.* 10(2):558–70.
23. Saura J, Tusell JM, Serratosa J. (2003) High-yield isolation of murine microglia by mild trypsinization. *Glia.* 44(3):183–89.
24. Chishti MA, Yang DS, Janus C, et al. (2001) Early-onset amyloid deposition and cognitive deficits in transgenic mice expressing a double mutant form of amyloid precursor protein 695. *J. Biol. Chem.* 276(24):21562–70.
25. Mengel D, Röskam S, Neff F, et al. (2013) Naturally occurring autoantibodies interfere with β-amyloid metabolism and improve cognition in a transgenic mouse model of Alzheimer's disease 24 h after single treatment. *Transl. Psychiatry.* 3: e236.
26. Dostal V, Link CD. (2010) Assaying β-amyloid toxicity using a transgenic C. elegans model. *J. Vis. Exp.* (44), e2252.
27. Wu Y, Wu Z, Butko P, et al. (2006). Amyloid-beta-induced pathological behaviors are suppressed by Ginkgo biloba extract EGb 761 and ginkgolides in transgenic Caenorhabditis elegans. *J. Neurosci.* 26(50):13102–113.
28. Bach JP, Mengel D, Wahle T, et al. (2011) The role of CNI-1493 in the function of primary microglia with respect to amyloid-β. *J. Alzheimers Dis.* 26(1):69–80.
29. Sakono M, Zako T. (2010) Amyloid oligomers: formation and toxicity of Abeta oligomers. *FEBS J.* 277(6):1348–58.
30. Kobro-Flatmoen A, Nagelhus A, Witter MP. (2016) Reelin-immunoreactive neurons in entorhinal cortex layer II selectively express intracellular amyloid in early Alzheimer's disease. *Neurobiol. Dis.* 93:172–83.
31. Link CD. (1995) Expression of human beta-amyloid peptide in transgenic Caenorhabditis elegans. *Proc. Natl. Acad. Sci. U.S.A.* 92(20):9368–72.
32. Metz JT, Hajduk PJ. (2010) Rational approaches to targeted polypharmacology: creating and navigating protein-ligand interaction networks. *Curr. Opin. Chem. Biol.* 14(4):498–504.
33. Braak H, Braak E. (1991) Neuropathological stageing of Alzheimer-related changes. *Acta. Neuropathol.* 82(4):239–59.
34. in t' Veld BA, Ruitenberg A, Hofman A, et al. (2001) Nonsteroidal antiinflammatory drugs and the risk of Alzheimer's disease. *N. Engl. J. Med.* 345(21):1515–21.
35. Breitner JC,Baker LD, Montine TJ, et al. (2011) Extended results of the Alzheimer's disease anti-inflammatory prevention trial. *Alzheimers Dement.* 7(4):402–11.
36. Schwartz M, Shechter R. (2010) Systemic inflammatory cells fight off neurodegenerative disease. *Nat. Rev. Neurol.* 6(7):405–10.
37. Baruch K, Deczkowska A, Rosenzweig N, et al. (2016) PD-1 immune checkpoint blockade reduces pathology and improves memory in mouse models of Alzheimer's disease. *Nat. Med.* 22(2):135–37.
38. DeGiorgio LA, Konstantinov KN, Lee SC, Hardin JA, Volpe BT, Diamond B (2001) A subset of lupus anti-DNA antibodies cross-reacts with the NR2 glutamate receptor in systemic lupus erythematosus. *Nat. Med.* 7(11):1189–93.
39. de Vries B, Steup-Beekman GM, Haan J, et al. (2010) TREX1 gene variant in neuropsychiatric systemic lupus erythematosus. *Ann. Rheum. Dis.* 69(10):1886–87.
40. Salloway S, Sperling R, Fox NC, et al. (2014) Two phase 3 trials of bapineuzumab in mild-to-moderate Alzheimer's disease. *N. Engl. J. Med.* 370(4):322–33.
41. Medzhitov R, Schneider DS, Soares MP. (2012) Disease tolerance as a defense strategy. *Science.* 335(6071):936–41.
42. Griciuc A, Serrano-Pozo A, Parrado AR, et al. (2013) Alzheimer's disease risk gene CD33 inhibits microglial uptake of amyloid beta. *Neuron.* 78(4):631–43.

43. Kleinberger G, Yamanishi Y, Suárez-Calvet M, et al. (2014) TREM2 mutations implicated in neurodegeneration impair cell surface transport and phagocytosis. *Sci. Transl. Med.* 6(243): 243ra286.
44. Merlini G, Bellotti V. (2003) Molecular mechanisms of amyloidosis. *N. Engl. J. Med.* 349(6):583–96.
45. Kastritis E, Wechalekar AD, Dimopoulos MA, et al. (2010) Bortezomib with or without dexamethasone in primary systemic (light chain) amyloidosis. *J. Clin. Oncol.* 28(6):1031–37.
46. Dimopoulos M, Spencer A, Attal M, et al. (2007) Lenalidomide plus dexamethasone for relapsed or refractory multiple myeloma. *N. Engl. J. Med.* 357(21):2123–32.
47. Coelho T, Adams D, Silva A, et al. (2013) Safety and efficacy of RNAi therapy for transthyretin amyloidosis. *N. Engl. J. Med.* 369(9):819–29.
48. Noelker C, Stuckenholz V, Reese JP, et al. (2013) CNI-1493 attenuates neuroinflammation and dopaminergic neurodegeneration in the acute MPTP mouse model of Parkinson's disease. *Neurodegener. Dis.* 12(2):103–10.

Cite this article as: Sankowski R, *et al*. (2016) The multi-target effects of CNI-1493: convergence of antiamylodogenic and antiinflammatory properties in animal models of Alzheimer's disease. *Mol. Med*. 22:776–88.